The effect of thermal core–mantle interactions on the palaeomagnetic secular variation

Jeremy Bloxham

Phil. Trans. R. Soc. Lond. A 2000 **358**, 1171-1179
doi: 10.1098/rsta.2000.0579

THE ROYAL SOCIETY

The effect of thermal core–mantle interactions on the palaeomagnetic secular variation

By Jeremy Bloxham

Department of Earth and Planetary Sciences, Harvard University, 20 Oxford Street, Cambridge, MA 02138, USA

We compare a numerical dynamo model with a model of the palaeosecular variation and find that, although there is good agreement in the meridional distribution of the secular variation, the amplitude of secular variation in the dynamo model is too small. Increasing the Rayleigh number does little to increase the amplitude of the secular variation, while it increases the axial dipole component of the field to geophysically unreasonably large values. However, by introducing lateral variations in heat flux across the core–mantle boundary into the dynamo model, we are able to match the amplitude of the secular variation. In addition, we find that the dynamo model then exhibits persistently anomalous behaviour beneath the Pacific region.

Keywords: geomagnetism; geodynamo; secular variation; core–mantle interactions

1. Introduction

Although there has been considerable progress in recent years in the development of dynamically self-consistent numerical models of the geodynamo (Glatzmaier & Roberts 1995*a*, *b*; Jones *et al.* 1995; Sarson *et al.* 1997; Kuang & Bloxham 1997, 1999), very great numerical challenges remain in attempting to understand the dynamo process through numerical models. Part of the problem stems from the range of time-scales on which the geomagnetic field varies: at the short period end of the spectrum are torsional oscillations with decadal periods; four or five orders of magnitude longer is the time-scale of geomagnetic reversals. Numerical models are not necessarily well suited to studying either of these extremes. At short periods, numerical dynamo models typically suffer from excessive viscous dissipation, so much of interest is simply damped out, while, on account of the computational expense of dynamo models, the time-span that they typically cover is short compared with that on which the field reverses.

However, the most important time-scales for the dynamo are the dipole free decay time-scale of *ca.* 20 000 yr and, arguably more important, the time-scale of convective overturn in the core of a few hundred years. Convection in the core also manifests itself in the secular variation, for which we have direct observations spanning roughly one convective turnover. These observations provide useful tests of dynamo models: we have previously compared a dynamo model with the directly observed record of secular variation over the last 300 yr (Kuang & Bloxham 1997, 1998).

Our aim in this paper is to compare a numerical dynamo model with the so-called palaeomagnetic secular variation, the secular variation as determined from palaeomagnetic measurements spanning the last 5 Myr. Typically, models of the palaeomagnetic secular variation describe the variance of the field about some time-averaged state, either an axial dipole or an axial dipole augmented by a small axial quadrupole. Even though the observations from which these models are derived span 5 Myr, the dominant process contributing to the palaeomagnetic secular variation—in other words, the process responsible for the departures of the field from the time-averaged state—is convection in the core on a much shorter time-scale. In fact, 5 Myr is chosen as the time-interval from which palaeomagnetic measurements are selected, not because of the time-scales of the secular variation but, instead, to obtain an adequate sampling of the field given the poor distribution of palaeomagnetic measurements; while if a longer time-interval than 5 Myr were chosen, then the complication of having to correct the observations for plate motions would arise.

So, although numerical dynamo models span much less than 5 Myr, the palaeomagnetic secular variation is a useful and important test of these models, since the dominant process that is represented by the palaeomagnetic secular variation, namely convection in the core, is one that the models should represent well.

2. The palaeomagnetic secular variation

We begin by contrasting models of the secular variation based on historical observations of the magnetic field with models based on palaeomagnetic measurements. Historical observations have the property that the time of each observation that is used to determine the model is known to an accuracy (typically less than one day) that is much better than the characteristic time-scale of the secular variation (a few hundred years). On the other hand, for palaeomagnetic observations, the time at which the magnetization was acquired is known only with a large uncertainty that is much greater than the dominant periods of the secular variation. As a result, historical observations can be used to produce deterministic models of the secular variation, while palaeomagnetic measurements must be considered as random samples of the secular variation from which the statistics of the secular variation can be derived.

The first such statistical description of the secular variation was the model CP88 of Constable & Parker (1988). The time-averaged field (after accounting for reversals) in their model consists of an axial dipole ($g_1^0 = -30\,000$ nT) and an axial quadrupole ($g_2^0 = 0.06 g_1^0$). The secular variation is isotropic, in other words, the variance of each coefficient about its mean is only a function of spherical harmonic degree l and is independent of spherical harmonic order m, so that the representation of the secular variation is invariant to rotations of the reference frame about the centre of the Earth.

Subsequent work showed that this isotropic model does not provide an adequate description of the secular variation (Kent & Smethurst 1995; Hulot & Gallet 1996; Johnson & Constable 1996; Quidelleur & Courtillot 1996). More recently, Constable & Johnson (1999) have extended CP88 by introducing axial anisotropy (model CJ98, in which the variances depend on both l and m, but not on the phase of the spherical harmonics) and general anisotropy (model CJ98.nz, in which the restriction on phase is relaxed).

For this study, we adopt model CJ98, which, like CP88, has a time-averaged axial dipole and axial quadrupole. Axial anisotropy is introduced in spherical harmonic degrees 1 and 2 by allowing the variance of order-1 terms to be different from the variance of the other terms of those degrees. In figure 1, we show the meridional

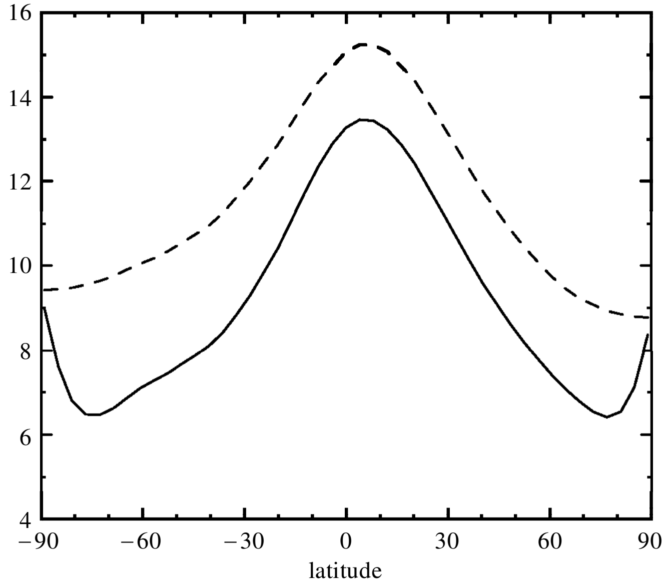

Figure 1. The meridional distribution of two field components derived from CJ98. The solid line shows the standard deviation of the inclination about an axial dipole; the dashed line shows the standard deviation of the field direction about an axial dipole.

distribution of two components derived from CJ98: the standard deviations in inclination and in total field direction (angular dispersion) between the field and an axial dipole field. We note that the standard deviation in inclination has more structure than that of field direction, and so we choose to use inclination for the comparisons that follow.

3. Comparison with a dynamo model with homogeneous boundary conditions

In figure 2, we compare CJ98 with the numerical dynamo model of Kuang & Bloxham (1997, 1998, 1999) over a period of 2.5 dipole decay times, or *ca.* 50 000 yr. As described in the aforementioned papers, the dynamo model is Boussinesq, has viscous stress-free boundary conditions, is driven thermally with heat flux boundary conditions at the inner core and core–mantle boundaries, and has an electrically finitely conducting inner core. The Ekman number and Rossby number both equal 2×10^{-5}. The Rayleigh number for the calculation referred to in figure 2 is 15 000, or about 35 times larger than the critical Rayleigh number for the onset of thermal convection; here, we have defined the Rayleigh number as

$$Ra = \alpha g h r_0^2 / 2\Omega\eta,$$

where α is the coefficient of thermal expansion, g the acceleration due to gravity, h the temperature gradient at the inner core boundary, r_0 the outer core radius, Ω the Earth's rotation rate, and η the magnetic diffusivity. It is immediately apparent from figure 2 that even though the meridional distribution of secular variation from the dynamo model has a similar shape to that of CJ98, the amplitude is substantially

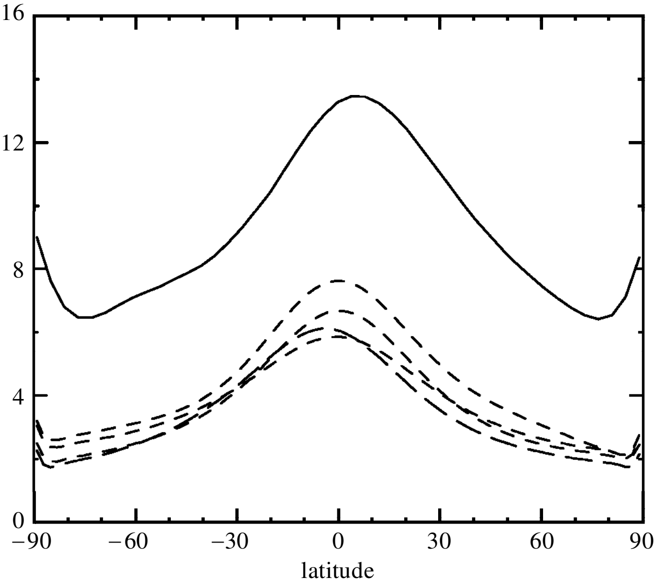

Figure 2. The meridional distribution of the standard deviation of the inclination about an axial dipole. The solid line is CJ98; the long-dashed line is the dynamo model; the shorter-dashed lines are the dynamo model at larger values of the Rayleigh number, with an increase of *ca.* 20% in Rayleigh number between each line.

smaller. The agreement in shape presumably reflects the fact that the dynamo model and the Earth have the same geometry.

We interpret this distribution as follows. We believe that the small increase in secular variation near the poles is due to the effect of the tangent cylinder (the cylinder tangent to the inner core boundary and co-axial with the rotation axis). This effect has previously been noted in maps of the magnetic field at the core–mantle boundary (Gubbins & Bloxham 1987). The other noteworthy feature of the plot is the more rapid increase in secular variation within *ca.* 45° of the Equator. We interpret this as being due to the occurrence of core spots within that region, resulting from expulsion of toroidal field from the core (Allan & Bullard 1966; Bloxham & Gubbins 1985).

One possible explanation of this discrepancy in amplitude is that the Rayleigh number is too small in the dynamo model. It is not unreasonable to expect that increasing the Rayleigh number would increase the strength of the secular variation. We note that for the dynamo model, the superadiabatic heat flux across the core–mantle boundary is *ca.* 10^{12} W, leaving considerable leeway for increasing the Rayleigh number. However, we should be mindful of the fact that given that these calculations are performed at values of the Ekman number much larger than that of the Earth's core, and given that the critical Rayleigh number scales as E^{-1} (Gubbins & Roberts 1987), the leeway for increasing the Rayleigh number will be restricted by the ratio of the Rayleigh number to the critical Rayleigh number. In figure 2, we show the results for four calculations: the original calculation and three at higher Rayleigh number, the Rayleigh number being increased by *ca.* 20% from one run to the next (the actual values of the Rayleigh number are 15 000, 18 000, 22 000 and 27 000). The effect on the amplitude of the secular variation is modest, but the effect on the amplitude of the magnetic field at the core–mantle boundary is large. The axial dipole scales almost linearly with the Rayleigh number (even though the mean field strength does not), leading to unreasonably strong axial dipole components. As the Rayleigh number is increased, the mean field strength should increase as $Ra^{1/2}$. However, the poloidal field strength (and, hence, the axial dipole) can increase more rapidly, since it is not in magnetostrophic balance and increasing the Rayleigh number increases the convective meridional circulation, thus enhancing the conversion of toroidal field to poloidal field.

An alternative explanation is needed for the discrepancy in amplitude seen in figure 2. One possibility, which we investigate in the next section, is that inhomogeneous thermal boundary conditions (lateral variations in heat flux at the core–mantle boundary) are required. Other possibilities, which we do not investigate, include the possibility that reducing the role of dissipative processes (especially viscous dissipation) might lead to more intense secular variation as smaller scales become more important.

4. A dynamo model with inhomogeneous boundary conditions

Maps of the magnetic field at the core–mantle boundary over the period 1715–1980 reveal that certain features in the field, in particular concentrations of flux at *ca.* 60° latitude (or flux lobes), remain at approximately the same longitude instead of drifting westward as would be expected (Gubbins & Bloxham 1987). Bloxham & Gubbins (1987) proposed that this behaviour is due to thermal core–mantle interactions, whereby lateral variations in temperature in the lowermost mantle result in lateral variations in heat flux across the core–mantle boundary, which influence the pattern of convection in the core. Some support for this suggestion comes from correlation between the predominantly Y_2^2 pattern of seismically inferred heterogeneity in the lowermost mantle (Giardini *et al.* 1987) and the pattern of flux lobes at the core–mantle boundary.

Further support for the importance of core–mantle interactions comes from palaeomagnetism. Maps of the magnetic field at the core–mantle boundary for the period 0–5 Ma derived from palaeomagnetic measurements show evidence of persistent non-zonal structure in the magnetic field (Gubbins & Kelly 1993; Johnson & Constable 1995, 1997; Kelly & Gubbins 1997). Additionally, palaeomagnetic measurements indicate that the magnetic field in the Pacific region has been persistently anomalous for the last 5 Myr, as most recently addressed by Johnson & Constable (1998). Neither of these observations would be expected given the much shorter time-scales characteristic of the dynamo.

Interactions between the core and mantle may take forms other than that described by Bloxham & Gubbins (1987). Hide (1969) was the first to suggest that core–mantle interactions will arise through the effect of topography on the core–mantle boundary (see also Gubbins & Richards 1986); other possible mechanisms of interaction include lateral variations in electrical conductivity (Jeanloz 1990) or lateral variations in thermal conductivity. Unfortunately, seismic tomography is ill equipped to help us distinguish between these. For example, seismically slow regions of the lowermost mantle can be interpreted in several ways. One interpretation is that they result from hotter-than-average thermal anomalies; then the magnitude of the temperature gradient at the core–mantle boundary (the core–mantle boundary itself is nearly isothermal) will be smaller than average, resulting in below-average heat flux from the core. An alternative explanation is that they result from regions in which the iron content of the perovskite lower mantle is higher than average, since increasing the iron content reduces seismic velocities (Birch 1961; Shankland 1972); however, increased iron content corresponds to increased thermal conductivity, and, hence, to above-average heat flux from the core. Interpretation in terms of topographic coupling is even more complicated since it involves such poorly known factors as the viscosity structure of the lowermost mantle (Gubbins & Richards 1986). Finally, lateral variations in electrical conductivity, although certainly present if there are significant lateral variations in the iron content of the lowermost mantle, are unlikely, owing to the short magnetic diffusion time-scale in the lowermost mantle, to be responsible for persistent features in the magnetic field on the time-scale of millions of years.

Here, we assume a thermal model for core–mantle interactions. We use a shear velocity model of the mantle (Masters *et al.* 1996) to derive lateral variations in heat flux at the core–mantle boundary on the dynamo model, with fast regions of the lowermost mantle corresponding to regions of high heat flux and slow regions to low heat flux. Given the uncertainty in interpretation of the seismic anomalies and the additional uncertainties that surround the composition and viscosity structure of the lowermost mantle, we have not attempted to scale the shear-velocity model to variations in heat flux. Instead, we have chosen an amplitude for the variations in heat flux that has a discernible influence on the dynamo while not totally dominating it. The RMS amplitude of the lateral variations in heat flux of 21% of the superadiabatic heat which we have used is certainly not geophysically unreasonably large. The boundary condition is implemented straightforwardly, though some care must be taken since the dynamo model is in a reference frame with constant rotation, within which the mantle rotates differentially.

The results are shown in figure 3, from which it is apparent that the amplitude discrepancy has, in large part, been resolved. We infer from this that the vigour of the palaeomagnetic secular variation is explained by thermal core–mantle interactions, though other explanations may also be possible.

As mentioned, additional evidence for thermal core–mantle interactions comes from persistently anomalous fields in the Pacific region. In figure 4 we show the departure of the inclination of this dynamo model from that of an axial dipole field. For this figure we have averaged the output of the dynamo model with lateral variations in heat flux over a 50 000 yr interval; the dynamo model without lateral variations in heat flux averaged almost perfectly to an axial dipole configuration over this time-span. It is apparent that the inclination anomaly in the Pacific region is smaller than the average inclination anomaly. We emphasize that this result pertains to the average field: in our model, we find that the average field beneath the Pacific is more nearly dipolar than elsewhere; we do not find that the secular variation (the rate of change of field) is, on average, different between the two hemispheres on this time-scale.

It is worth noting that the terms 'nearly dipolar' and 'low secular variation' are not necessarily synonymous, and that to distinguish between them with data that are poorly distributed in space and time is not straightforward.

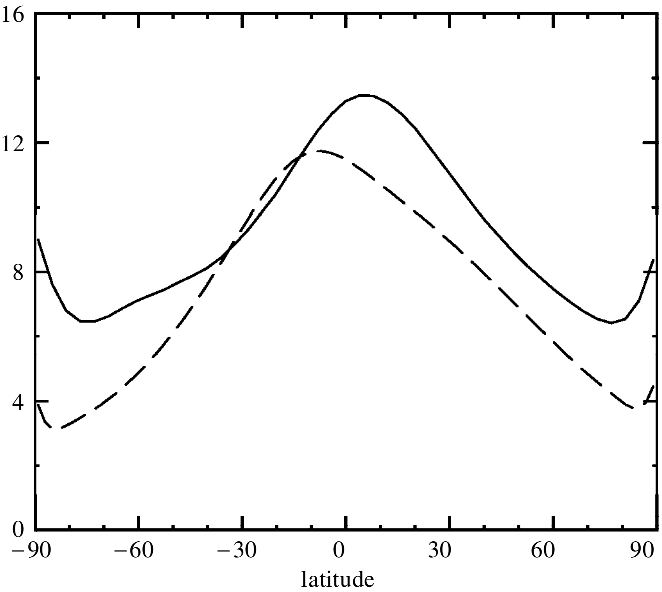

Figure 3. The meridional distribution of the standard deviation of the inclination about an axial dipole. The solid line is CJ98, the dashed line is the dynamo model with lateral variations in heat flux.

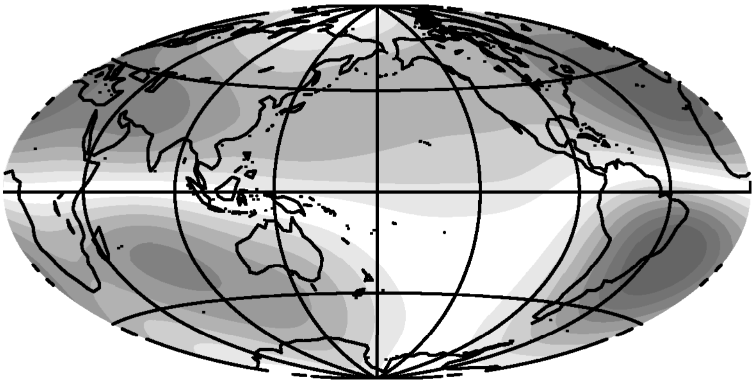

Figure 4. The difference in inclination between a 50 000 yr average of the dynamo model with lateral variations in heat flux and an axial dipole. The greyscale is in increments of 1°. Note that the time-averaged field is more nearly dipolar in the Pacific region than elsewhere.

Finally, we consider the original evidence for thermal core–mantle interactions, namely, persistent flux lobes. Here, the situation is more complicated and will be reported on in more detail elsewhere. Briefly though, we do not find persistent flux lobes on the 50 000 yr time-scale of this calculation. Instead, we see intermittent behaviour with flux lobes appearing at high latitude, only to be eventually advected away by the flow. Such intermittent behaviour has been reported previously in the non-magnetic case by Zhang & Gubbins (1993, 1997) and by Sarson *et al.* (1997) in the first such study to use a dynamically self-consistent dynamo model. In a study of magnetoconvection with lateral variations in heat flux, Olson & Glatzmaier

(1996) found that lateral variations in heat flux broke the columnar nature of the convection, seemingly in contrast with the observed near symmetry of flux lobes about the Equator, but possibly explained by the extremely large value that they adopted for the ratio of the Rayleigh number to the critical Rayleigh number.

5. Discussion

The palaeomagnetic secular variation provides a useful set of constraints on numerical models of the geodynamo. We find that we are able to reproduce the meridional distribution of the secular variation well by incorporating lateral variations in heat flux at the core–mantle boundary into our dynamo model, suggesting that core–mantle interactions play an important role in determining the visor of the secular variation. In addition, we find a persistent difference between the Pacific and Atlantic hemispheres, something that we had observed only for short periods (a few hundred years) in the model without lateral variations in heat flux (Kuang & Bloxham 1998).

Much remains to be done to understand the behaviour of flux lobes at high latitude in our dynamo model and in geomagnetic field models. Geomagnetic field models show some indications of intermittency, possibly resulting from interactions between travelling waves and the flux lobes (Bloxham *et al.* 1989). However, high-resolution palaeomagnetic measurements from sediment cores probably hold the greatest promise for constraining the long-term behaviour of the flux lobes.

The author is very grateful to Cathy Constable and Catherine Johnson for kindly providing a preprint of their work and for useful discussions, and to Guy Masters, who kindly provided a copy of the shear-velocity model used in this study. This work was supported by the NSF.

References

Allan, D. W. & Bullard, E. C. 1966 The secular variation of the Earth's magnetic field. *Proc. Camb. Phil. Soc.* **62**, 783–809.

Birch, F. 1961 The velocity of compressional waves in rocks to 10 kilobars. *J. Geophys. Res.* **66**, 2199–2224.

Bloxham, J. & Gubbins, D. 1985 The secular variation of the Earth's magnetic field. *Nature* **317**, 777–781.

Bloxham, J. & Gubbins, D. 1987 Thermal core–mantle interactions. *Nature* **325**, 511–513.

Bloxham, J., Gubbins, D. & Jackson, A. 1989 Geomagnetic secular variation. *Phil. Trans. R. Soc. Lond.* A **329**, 415–502.

Constable, C. G. & Johnson, C. L. 1999 Anisotropic paleosecular variation models: implications for geomagnetic field observables. *Phys. Earth Planet. Interiors* **115**, 35–51.

Constable, C. G. & Parker, R. L. 1988 Statistics of the geomagnetic secular variation for the past 5 Ma. *J. Geophys. Res.* **93**, 11 569–11 581.

Giardini, D., Li, X.-D. & Woodhouse, J. 1987 Three-dimensional structure of the Earth from splitting in free-oscillation spectra. *Nature* **325**, 405–411.

Glatzmaier, G. A. & Roberts, P. H. 1995*a* A three-dimensional convective dynamo solution with rotating and finitely conducting inner core and mantle. *Phys. Earth Planet. Interiors* **91**, 63–75.

Glatzmaier, G. A. & Roberts, P. H. 1995*b* A three-dimensional self-consistent computer simulation of a geomagnetic field reversal. *Nature* **377**, 203–209.

Gubbins, D. & Bloxham, J. 1987 Morphology of the geomagnetic field and implications for the geodynamo. *Nature* **325**, 509–511.

Gubbins, D. & Kelly, P. 1993 Persistent patterns in the geomagnetic field over the past 2.5 Myr. *Nature* **365**, 829–832.

Gubbins, D. & Richards, M. 1986 Coupling of the core dynamo and mantle—thermal or topographic. *Geophys. Res. Lett.* **325**, 1521–1524.

Gubbins, D. & Roberts, P. H. 1987 Magnetohydrodynamics of the Earth's core. In *Geomagnetism* (ed. J. A. Jacobs), ch. 1, vol. 2, pp. 1–183. Academic.

Hide, R. 1969 Interaction between the Earth's liquid core and solid mantle. *Nature* **222**, 1055–1056.

Hulot, G. & Gallet, Y. 1996 On the interpretation of virtual geomagnetic pole (VGP) scatter curves. *Phys. Earth Planet. Interiors* **95**, 37–53.

Jeanloz, R. 1990 The nature of the Earth's core. *A. Rev. Earth Planet. Sci.* **18**, 357–386.

Johnson, C. L. & Constable, C. G. 1995 The time-averaged geomagnetic field as recorded by lava flows over the past 5 Myr. *Geophys. J. Int.* **122**, 485–519.

Johnson, C. L. & Constable, C. G. 1996 Paleosecular variation recorded by lava flows over the last 5 Myr. *Phil. Trans. R. Soc. Lond.* A **354**, 89–141.

Johnson, C. L. & Constable, C. G. 1997 The time-averaged geomagnetic field: global and regional biases for 0–5 Ma. *Geophys. J. Int.* **131**, 643–666.

Johnson, C. L. & Constable, C. G. 1998 Persistently anomalous Pacific geomagnetic fields. *Geophys. Res. Lett.* **25**, 1011–1014.

Jones, C. A., Longbottom, A. W. & Hollerbach, R. 1995 A self-consistent convection driven geodynamo model using a mean field approximation. *Phys. Earth Planet. Interiors* **92**, 119–141.

Kelly, P. & Gubbins, D. 1997 The geomagnetic field over the past 5 Myr. *Geophys. J. Int.* **128**, 315–330.

Kent, D. V. & Smethurst, M. A. 1995 Mapping the Gauss coefficients to the pole and models of paleosecular variation. *J. Geomag. Geoelctr.* **47**, 115–130.

Kuang, W. & Bloxham, J. 1997 An Earth-like numerical dynamo model. *Nature* **389**, 371–374.

Kuang, W. & Bloxham, J. 1998 Numerical dynamo modeling: comparison with the Earth's magnetic field. In *The core–mantle boundary region* (ed. M. Gurnis, M. Wysession, E. Knittle & B. Buffett), pp. 197–208. Geophysical Monograph. AGU.

Kuang, W. & Bloxham, J. 1999 Numerical modelling of magnetohydrodynamic convection in a rapidly rotating spherical shell: weak and strong field dynamo action. *J. Comp. Phys.* **153**, 51–81.

Masters, G., Johnson, S., Laske, G. & Bolton, H. 1996 A shear-velocity model of the mantle. *Phil. Trans. R. Soc. Lond.* A **354**, 1385–1410.

Olson, P. & Glatzmaier, G. A. 1996 Magnetoconvection and thermal coupling of the Earth's core and mantle. *Phil. Trans. R. Soc. Lond.* A **354**, 1413–1424.

Quidelleur, X. & Courtillot, V. 1996 On low degree spherical harmonic models of paleosecular variation. *Phys. Earth Planet. Interiors* **95**, 55–77.

Sarson, G. R., Jones, C. A. & Longbottom, A. W. 1997 The influence of boundary region heterogeneities on the geodynamo. *Phys. Earth Planet. Interiors* **101**, 13–32.

Shankland, T. J. 1972 Velocity–density systematics: derivation from Debye theory and the effect of ionic size. *J. Geophys. Res.* **77**, 3750–3758.

Zhang, K. & Gubbins, D. 1993 Convection in a rotating spherical fluid shell with an inhomogeneous temperature boundary condition at infinite Prandtl number. *J. Fluid Dyn.* **250**, 209–232.

Zhang, K. & Gubbins, D. 1997 Nonlinear aspects of core–mantle interaction. *Geophys. Res. Lett.* **20**, 2969–2972.